International Journal of Thermophysics, Vol. 28, No. 2, April 2007 (© 2007)
DOI: 10.1007/s10765-007-0159-1

Factors Affecting the Coverage Dependence of the Diffusivity of One Metal over the Surface of Another

P. Wynblatt,[1,2] D. Chatain,[3] A. Ranguis,[3] J.P. Monchoux,[3,4] J. Moon,[1,5] and S. Garoff[6]

Various factors that can affect the coverage dependence of diffusivity for the case of surface hetero-diffusion have been analyzed. Simple Monte Carlo modeling of the diffusion process shows that diffusivity can either increase or decrease with coverage, depending on whether the interaction between diffusing atoms is repulsive or attractive. The results of more detailed simulations show that these simple predictions are reasonable. If the diffusing species undergoes first-order phase transitions as a function of coverage, then important perturbations of the diffusion profiles will result. One final factor in coverage dependence of diffusivity is considered, namely, the possible effects of coverage on the surface step structure. An analysis of diffusion profiles obtained for the spreading of Bi over Cu(100) shows that the major effects of coverage on diffusivity come about from the presence of phase transitions, and from the inherent coverage dependence of diffusivity in systems with short-range repulsion.

KEY WORDS: bismuth; coverage dependence of diffusivity; Cu(100) surface; surface hetero-diffusion.

[1]Department of Materials Science and Engineering, Carnegie Mellon University, Pittsburgh, Pennsylvania 15213, U.S.A.
[2]To whom correspondence should be addressed. E-mail: pw01@andrew.cmu.edu
[3]CRMCN-CNRS, Campus de Luminy, 13288 Marseille cedex 9, France.
[4]Present address: CEMES, 31055 Toulouse cedex 4, France.
[5]Electronics and Telecommunication Research Institute, Daejeon 305-350, Korea.
[6]Physics Department, Carnegie Mellon University, Pittsburgh, Pennsylvania 15213, U.S.A.

1. INTRODUCTION

Although there has been a great deal of work aimed at the investigation of surface diffusion in metallic systems, the majority of that work has been devoted to measurements of surface self-diffusion. In contrast, considerably less work has been performed on the diffusion of one metallic species over another, i.e., surface hetero-diffusion. Much of the work on surface hetero-diffusion has been summarized in reviews by Gomer [1], Seebauer and Allen [2], and Nauvomets [3]. More recent studies have tended to focus on the diffusion of either Pb or Bi over Cu surfaces of different orientation [4–8].

Several factors have contributed to the choice of these Cu-based systems as convenient model systems for surface hetero-diffusion studies. The Pb–Cu and Bi–Cu bulk binary phase diagrams display negligible mutual solubilities of the components in the solid state. This feature ensures that as Pb or Bi diffuse over Cu surfaces, there is essentially no loss of the diffusing species from the surface by diffusion into the bulk. In addition, the vapor pressures of Pb and Bi at temperatures below their melting points are sufficiently low, such that no loss of the diffusing species can occur by evaporation into the gas phase. Finally, bulk three-dimensional (3D) Pb or Bi islands deposited on Cu surfaces, co-exist in equilibrium with 2D adsorbed layers of about monolayer thickness. An example

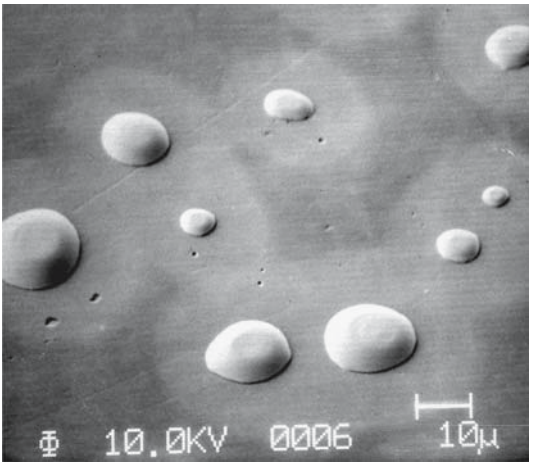

Fig. 1. Photomicrograph of 3D Pb particles on a Cu(111) substrate taken in a SAM. Particles are surrounded by halos of the spreading 2D adsorbed phase [6].

illustrating this type of coexistence is shown in Fig. 1 [6]. Thus, surface hetero-diffusion can conveniently be studied in these systems by measuring the rate of spreading of adsorbed monolayers from 3D sources. In particular, it is possible to determine coverage profiles in the 2D layer by Auger line scans acquired in a scanning Auger microscope (SAM) [6–8]. Such data allow the determination of diffusion coefficients, as well as coverage dependence of these diffusion coefficients in the 2D layer.

The diffusion coefficients of Pb and Bi over Cu substrates of various orientations have been found to be strongly dependent on the coverage of the diffusing species [4–8]. In many cases, the changes in diffusivity with coverage have been ascribed to the existence of different structures of the adsorbed species at different coverages, i.e., to the existence of surface phase transitions as a function of coverage. However, there are other factors that can lead to coverage dependence of diffusivity. Thus, the main focus of this paper will be to identify and discuss the principal factors that may play a role in the coverage dependence of diffusivity in surface hetero-diffusion. This will be accomplished by presenting selected results from previous studies of Bi diffusion over a Cu(100) surface [8], as well as from computer simulations of surface hetero-diffusion.

2. DIFFUSION PROFILE OF Bi OVER Cu(100)

For the case of Bi diffusion over Cu(100), spreading was studied from a 3D Bi film about $1\,\mu$m thick, deposited on the single crystal Cu substrate [8]. Composition profiles were obtained by line scans acquired in a SAM. The slab-like source geometry produced a 1D diffusion gradient, unlike the cylindrical spreading geometry illustrated in Fig. 1. Such a geometry simplifies the analysis of the resulting diffusion profiles. A sample experimental profile is shown in Fig. 2, where a coverage of one monolayer (θ = 1 ML) is defined as the maximum coverage in equilibrium with the 3D Bi deposit ($9.18\times10^{18}\,\text{atoms}\cdot\text{m}^{-2}$).

The figure shows that the profile is quite complex. This is typical of Pb and Bi profiles on Cu surfaces. The interpretation of such profiles has relied at least in part on a knowledge of the different surface structures that are known to exist at different values of coverage. However, there are several other phenomena that can affect the shape of surface hetero-diffusion profiles. These will now be described.

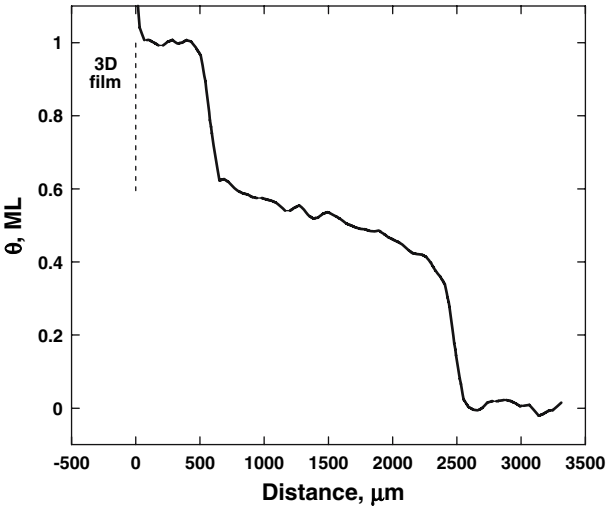

Fig. 2. Example of Bi coverage on Cu(100) versus distance measured from the edge of the 3D Bi film, obtained after heating at 513 K for 70 h [8].

3. COVERAGE DEPENDENCE OF DIFFUSIVITY

3.1. Expectations from a Simple Rigid Lattice Monte Carlo Model

Murch and Thorn [9] developed a rigid lattice Monte Carlo model to investigate the coverage dependence of diffusivity in 2D layers. The original model was formulated for diffusion of hetero-atoms over a substrate with a 2D honeycomb lattice. Here we have rewritten the model for diffusion over a square lattice, as shown in Fig. 3.

In the model, diffusing adatoms can only jump into unoccupied (vacant) adjacent sites. They interact with nearest neighbor diffusing adatoms with an energy ε, which is taken to be positive for attractive interactions, and negative for the case of repulsive interactions. An effective temperature, T^*, is defined by $T^* = kT/\varepsilon$. Lastly, the activation energy for a jump is assumed to depend on the coordination number of the jumping adatom. Thus, when repulsive interactions prevail, the neighbors of a jumping adatom tend to "push" the diffusing adatom over the activation barrier, thereby effectively reducing its height. The higher is the number of neighbors, the greater is the reduction of the activation barrier. Conversely, in the case of attractive interactions, it is assumed that the neighbors of the jumping adatom will tend to "hold back" the atom as it

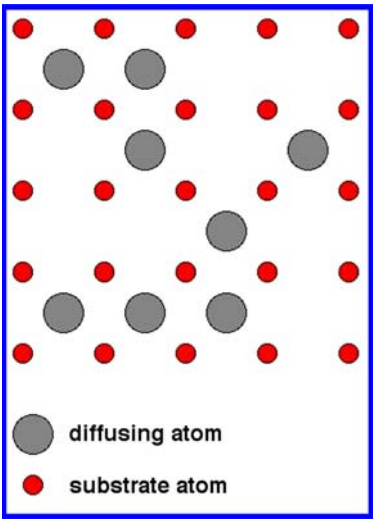

Fig. 3. Schematic of a square substrate lattice with a partial monolayer of diffusing species.

attempts to cross the barrier, thereby increasing the effective barrier height. More details are provided in the paper of Murch and Thorn [9].

By performing Monte Carlo simulations for specified values of T^* and the coverage, θ (taken to be the fraction of substrates sites occupied by diffusing atoms), it is possible to calculate three parameters of the diffusion process: V, the probability that a site adjacent to the jumping atom will be vacant; W, an effective atomic jump frequency; and f, a diffusion correlation factor. For a given value of T^*, these parameters are all functions of the coverage. In Fig. 4 we display a plot of $D(\theta)/D(0)$, defined by

$$\frac{D(\theta)}{D(0)} = \frac{V(\theta)W(\theta)f(\theta)}{V(0)W(0)f(0)} \tag{1}$$

Figure 4 shows that repulsive interactions tend to produce an increasing diffusivity with increasing coverage, and that attractive interactions tend to produce a decreasing diffusivity with increasing coverage. Furthermore, the effects of coverage depend on temperature, and can amount to changes in diffusivity exceeding an order of magnitude. Whereas this type of model can indicate some general trends, it neglects many important features of the diffusion process, such as the effects of local atomic relaxation, the presence of coverage (i.e., concentration) gradients, as well as the

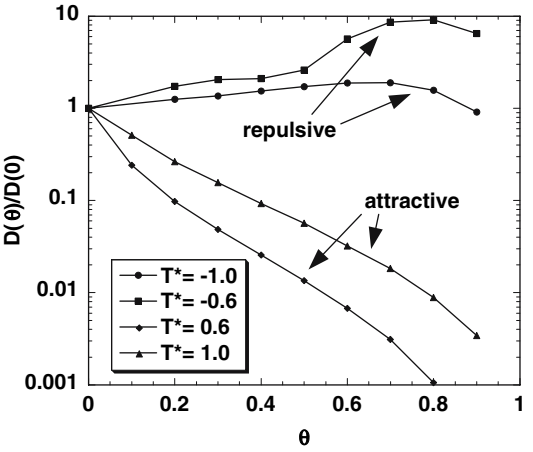

Fig. 4. Dependence of diffusivity on coverage calculated by the modified Murch and Thorn [9] model, for both attractive and repulsive interactions at different values of T^*.

possibility that adatoms are intermixed with substrate atoms in the diffusing layer, a phenomenon referred to as "surface alloying," that is discussed in greater detail below.

3.2. Molecular Dynamics Simulations with Embedded Atom Method Potentials

The coverage dependence of diffusivity has also been investigated by more sophisticated computer simulation approaches, such as molecular dynamics simulations [10], performed in conjunction with interatomic interactions described by embedded atom method (EAM) potentials [11]. This approach was used to investigate trends in the coverage dependence of diffusivity, for the case of Ag diffusing over Ni. The use of this methodology eliminates many of the deficiencies of rigid lattice Monte Carlo simulations, as it accounts for realistic local configurations, and was used to obtain coverage dependence of diffusivities in the presence of a concentration gradient. The Ag on Ni system was selected as a model system because it possesses one important property of the experimental systems, namely, an essential absence of mutual solubility.

The study simulated an Ag adsorbed layer spreading away from a slab-like 3D Ag film on a Ni(100) substrate. In these simulations, no surface alloying of the diffusing Ag adatoms with the substrate Ni atoms

was found to occur. An example of a coverage profile in the 2D layer is shown in Fig. 5. The fact that the profile does not display a classical error function shape is evidence of a coverage-dependent diffusivity. The dependence of diffusivity on coverage can be extracted from a profile of the type shown in Fig. 5 by the so-called Matano analysis [12], in which $D(\theta)$ is expressed as

$$D(\theta) = -\frac{1}{2t}\left(\frac{\mathrm{d}x}{\mathrm{d}\theta}\right)_{\theta}\int_0^{\theta} x\,\mathrm{d}\theta \tag{2}$$

where t is the time, x is the distance, and θ is the coverage, or a suitably normalized coverage. Application of the Matano analysis to Fig. 5 yields the coverage-dependent diffusivity displayed in Fig. 6. That figure shows that there is approximately one order of magnitude change in the diffusivity over the range of coverage from 0 to about one monolayer. The general trend shown in Fig. 6 is similar to the trends shown in Fig. 4 for the simple Monte Carlo model for the case of repulsive interactions. For the case of Ag on Ni, the EAM potentials used are consistent with short-range repulsive interactions, although at long range, interactions become attractive. However, from the standpoint of the detailed interactions during a diffusive jump, short-range interactions are expected to play a much more significant role. For the case of experiments with Pb or Bi on Cu,

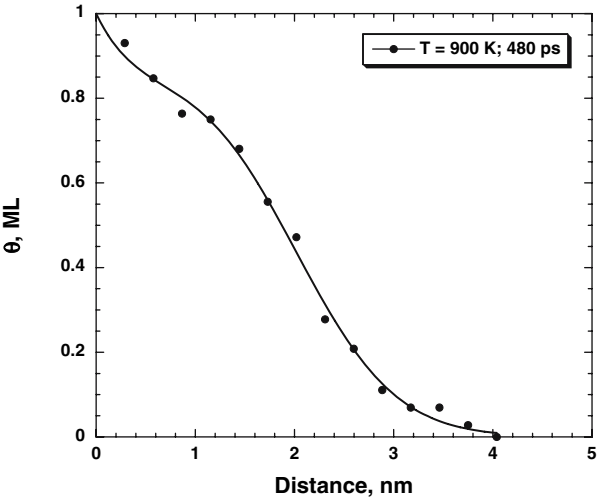

Fig. 5. Example of Ag profile on Ni(100) obtained by molecular dynamics simulation at $T = 900\,\mathrm{K}$, for a simulation time of 480 ps [10].

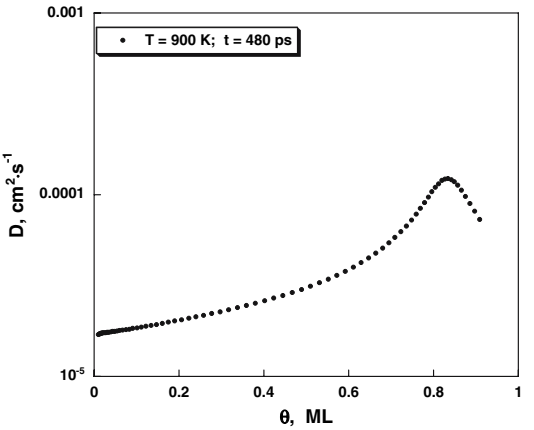

Fig. 6. Coverage dependence of diffusivity calculated from the profile of Fig. 5.

the diffusing species have a much larger atomic radius than the substrate atoms, as is also the case for Ag on Ni. As a result, one expects that strong repulsive interactions will occur at short range, so that an increasing diffusivity with increasing coverage is expected in all these cases.

3.3. Surface Phase Transitions

The occurrence of first-order surface phase transitions with changes in coverage, or more specifically, the presence of regions of phase coexistence in the surface phase diagram, can lead to abrupt coverage (concentration) changes in diffusion profiles (see Ref. [1] for surface diffusion, and Ref. [13] for volume diffusion). In order to evaluate these effects, we consider the phase diagram of Bi on Cu(100) as shown in Fig. 7a. This phase diagram has been inferred [8] from several recent literature reports of the surface phases present as a function of coverage [14–16]. Although the measurements underlying Fig. 7a have been performed over a temperature range extending from room temperature to ~550 K, no significant variation of the phase boundaries with temperature have been found. We have therefore ignored temperature effects in the phase diagram of Fig. 7a, as well as in the following discussion.

The Bi–Cu(100) surface phase diagram displays four phases with the following structures: p(10×10), c($9\sqrt{2} \times \sqrt{2}$)R45°, c($2 \times 2$), and a 2D lattice gas phase, at progressively decreasing Bi coverage. These phases will henceforth be abbreviated: p10, c9, c2, and LG. Two domains of two-phase coexistence are shown, one between the c9 and c2 phases, and the

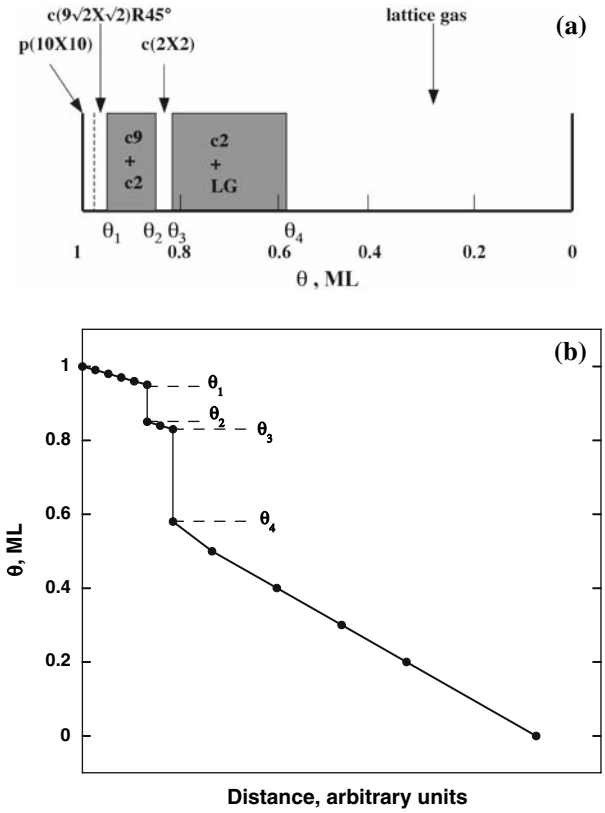

Fig. 7. (a) Surface phase diagram for Bi on Cu(100) and (b) schematic diffusion profile corresponding to (a).

other between the c2 and LG phases. Thus, the c9 to c2 and the c2 to LG transitions are first-order. Evidence on the nature of the transition between p10 and c9 is not definitive, so we have indicated the transition by a dashed line in Fig. 7a.

The p10, c9, and c2 structures are all similar. Both the p10 and c9 structures consist of blocks of c2 separated by 1D stacking faults in which the Bi density is somewhat higher than in the c2 structure, thus leading to a higher Bi coverage in those phases. The p10 structure possesses two perpendicular sets of faults, whereas the c9 structure has only one.

One additional difference between the various Bi phases on Cu(100) needs to be noted. The low coverage LG phase is surface alloyed, i.e., Bi atoms are incorporated into the topmost Cu surface layer. In contrast, the

other phases are "dealloyed," i.e., the Bi atoms are present in a distinct layer above the Cu substrate, and no significant number of Cu atoms are present in the Bi layer. Figure 7b shows a schematic composition profile corresponding to the phase diagram. For the purposes of this illustration, it has been assumed that the diffusion coefficients of Bi in all phases are approximately equal, and that there is no coverage dependence in any of the phases. The compositions corresponding to the ranges of coexistence of the c9 and c2 phases, and of the c2 and LG phases (i.e., between θ_1, and θ_2, and between θ_3 and θ_4, respectively) will not appear on the diffusion profile, as these regions of phase coexistence are adequately represented on the sample by the interfaces between the phases c9 and c2, and c2 and LG. Thus, in general, any region of phase coexistence is expected to be absent from a diffusion profile, thereby leading to an abrupt change in coverage [1,13]. However, there are many reasons that can lead to less abrupt changes in coverage in an experimental profile, than those shown in Fig. 7b. These include, for example, the resolution of the measurement compared to the distance over which the interface wanders, the presence of surface roughness, etc. Under these conditions, the measured variation in coverage would be somewhat smoothed out.

3.4. Activation Barriers at Surface Steps

No surface is atomically flat over the distances investigated in a typical diffusion experiment (10^2 to 10^3 μm). A typical scanning tunneling microscopy image of the Cu(100) surface, with either low or no Bi coverage, is displayed in Fig. 8. The figure shows that the surface roughness amounts to height differences of about 3 nm over distances of 500 nm, and that many monoatomic steps are therefore present at the surface. Diffusion across the edge of surface steps may be associated with a diffusion activation barrier (known as the Ehrlich–Schwoebel barrier [17,18]), which can be higher than the activation barrier between the sites of the flat surface terraces. In general, the presence of Ehrlich–Schwoebel barriers does not lead to a coverage dependence of diffusivity, although it can affect the observed activation energy for diffusion, and hence the diffusivity. However, if a change in coverage of the diffusing species can modify the structure of the surface steps, then there can also be a related change in diffusivity. This is indeed what seems to happen for the case of Bi on Cu.

3.5. Microfacetting of Cu(100) under High Bi Coverage

The equilibrium crystal shape (ECS) of pure Cu displays all possible crystallographic orientations [19], i.e., Cu surfaces of all orientations

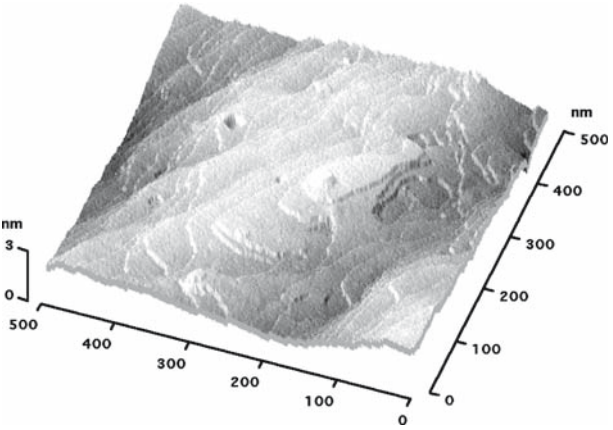

Fig. 8. STM image showing surface topography of Cu(100) surface used for diffusion studies.

are stable. In contrast, the ECS of Bi-saturated Cu displays only {111}, {100}, {320}, and {110} facets [20], thereby indicating that all surfaces orientations, except for these facet orientations, are unstable. The ECS of Bi-saturated Cu is displayed in Fig. 9. The figure shows that any local deviation of surface orientation from {100} will lead to the bunching of surface steps to form {320} microfacets. Although the ECS of Bi-saturated Cu was determined at 1223 K, well above the temperature of the diffusion experiment (513 K), we find that regions of the Cu(100) surface with maximum Bi coverage, held at 513 K for a few hours, do tend to microfacet, as shown in the STM photomicrograph of Fig. 10. An analysis of the angle between the microfacets in Fig. 10 yields an estimated orientation of {310} for the new microfacets. This difference between the microfacet orientations in equilibrium with {100}, obtained at 1223 and 513 K, could be due either to real differences between the ECS of Bi-saturated Cu at these two temperatures, or to kinetic effects resulting is slower equilibration of the Bi-saturated surface at 513 K. However, whether the differences are due to equilibrium or to kinetic reasons, the fact remains that there are significant differences in surface morphology of the Cu surface, depending on whether the Bi coverage is low (Fig. 8) or high (Fig. 10). Thus, the diffusivity measured at high Bi-coverage will be the result of diffusion not only over {100} orientations, but also partly over surfaces of {310} orientations. This could clearly have some effect on the measured diffusivity as a function of coverage.

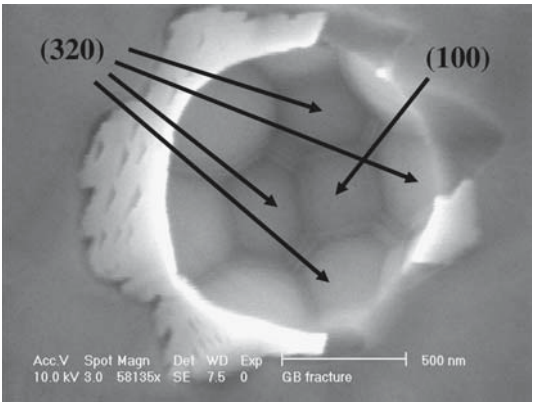

Fig. 9. Partially equilibrated grain boundary pore in Bi-saturated Cu, showing equilibrium facets. Note that {100} facets are surrounded by {320} facets and/or {320} microfacets [20].

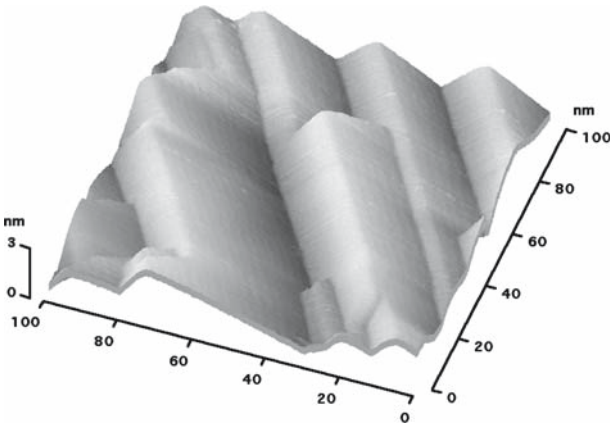

Fig. 10. STM micrograph of high Bi-coverage region of Cu(100) crystal, showing formation of {310} microfacets.

4. COVERAGE DEPENDENCE OF Bi DIFFUSIVITY OVER Cu(100)

The coverage dependence of the diffusivity of Bi over Cu(100) had been obtained by applying the Matano analysis of Eq. (2) to several profiles such as Fig. 2, and averaging the results [8]. This procedure yields $D(\theta)$ as displayed in Fig. 11. The figure shows a strong dependence of diffusivity on coverage, ranging over about three orders of magnitude.

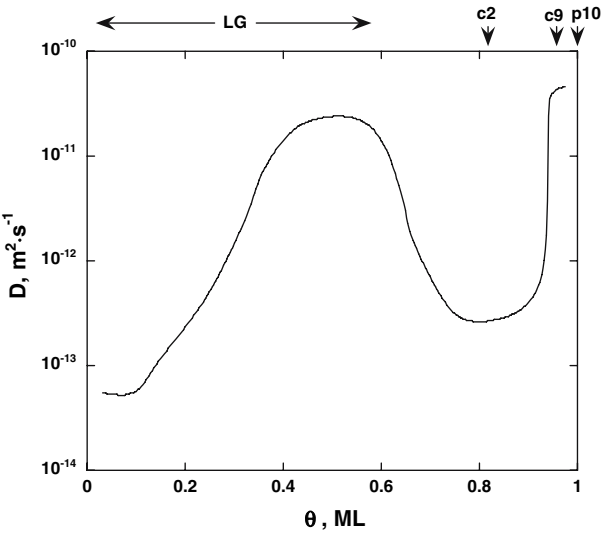

Fig. 11. Coverage dependence of diffusivity for Bi on Cu(100) obtained by a Matano analysis of data such as Fig. 2 [8].

A major effect on the appearance of experimental profiles comes from the presence of structural phase transitions as a function of coverage, as can be seen by comparing Fig. 2 with Fig. 7b. However, there are two important differences between those figures. First, the schematic of Fig. 7b shows a step on the profile in the vicinity of 0.8 ML where the c2 phase is present. It should be recalled that Fig. 7b was drawn under the assumption that the diffusivities in all the phases was approximately equal. However, Fig. 11 shows that the diffusivity in the c2 phase is considerably smaller than that in the p10, c9, and the high coverage end of the LG phase. Under these conditions, the offset of the profile associated with the c2 phase is experimentally undetectable. A second difference between Figs. 2 and 7b is the presence of an abrupt termination of the experimental profile as the coverage in the LG phase approaches zero, which is not seen in the schematic of Fig. 7b. Again, if one refers to Fig. 11, this feature is seen to be associated with a rapidly decreasing diffusivity in the LG phase as the coverage approaches zero. The LG phase is the only one which possesses a large domain of existence (from about 0.6 to 0 ML), and this strong dependence of diffusivity with coverage in the LG phase is most likely related to the general effects of coverage on diffusivity that were modeled in Sections 3.1 and 3.2 above. In contrast, the coverage range over which

the p10, c9, and c2 phases exist is too narrow for the effects of coverage variation on diffusivity to become obvious.

It should be emphasized, however, that the models of Sections 3.1 and 3.2 are strictly applicable to diffusion in dealloyed layers of adatoms, and do not therefore account for the surface alloyed nature of the LG Bi-phase. Thus, they may not capture the additional complexities that could arise in surface alloyed layers, where the movement of Bi atoms also requires the movement of Cu atoms. Such details of the diffusion processes in surface alloyed phases have been identified in recent studies [21–23], but are beyond the scope of this paper.

Figure 11 shows that diffusivity of Bi through the p10 and c9 structures is considerable higher than through the c2 structure. As mentioned earlier, these three structures are similar in that the p10 and c9 structures consist of c2 blocks separated by 2D stacking faults. Thus, one can conclude that the higher diffusivity in the p10 and c9 structures is most likely due to a much higher mobility of Bi atoms through the faulted regions than through the well-ordered c2 regions.

5. SUMMARY

An analysis of features which can affect the coverage dependence of diffusivity has been given. Some general trends of decreasing diffusivity with decreasing coverage can be inferred from simple rigid lattice Monte Carlo simulations for cases where repulsive interactions prevail between diffusing atoms in dealloyed layers. The results of more detailed simulations show that these simple predictions are reasonable. However, if the diffusing system undergoes first-order phase transitions over the coverage range of study, then important perturbations of the diffusion profiles can result. An analysis of diffusion profiles obtained for the spreading of Bi over Cu(100) shows that the major effects of coverage on diffusivity come about from the presence of phase transitions, as well as possibly from the inherent coverage dependence of diffusivity in systems with short-range repulsion. Another possible origin of coverage dependence has been discussed, namely, the effects of changes in the step structure that can result from changes in coverage. No specific evidence for these effects has been found.

REFERENCES

1. R. Gomer, *Rep. Prog. Phys.* **53**:917 (1990).
2. E. G. Seebauer and C. E. Allen, *Prog. Surf. Sci.* **49**:265 (1995).
3. A. G. Nauvomets, *Physica A* **357**:189 (2005).

4. C. Cohen, Y. Girard, P. Leroux-Hugon, A. L'Hoir, J. Moulin and D. Schmaus, *Europhys. Lett.* **24**:767 (1993).
5. G. Prévot, C. Cohen, J. Moulin and D. Schmaus, *Surf. Sci.* **421**:364 (1999).
6. J. Moon, J. Lowekamp, P. Wynblatt, S. Garoff and R. M. Suter, *Surf. Sci.* **488**:73 (2001).
7. J. Moon, P. Wynblatt, S. Garoff and R. M. Suter, *Surf. Sci.* **599**:160 (2004).
8. J. P. Monchoux, D. Chatain and P. Wynblatt, *Surf. Sci.* **600**:1265 (2006).
9. G. E. Murch and R. J. Thorn, *Philos. Mag.* **35**:493 (1977).
10. J. Moon, J. Yoon, P. Wynblatt, S. Garoff and R. M. Suter, *Comput. Mater. Sci.* **25**:503 (2002).
11. S. M. Foiles, M. I. Baskes and M. S. Daw, *Phys. Rev. B* **53**:7983 (1986).
12. J. Crank, *The Mathematics of Diffusion* (Clarendon Press, Oxford, 1956).
13. Y. Adda and J. Philibert, *La Diffusion dans les Solides* (Institut National des Sciences et Techniques Nucléaires, Saclay, 1966).
14. H. L. Meyerheim, H. Zajonz, W. Moritz and I. K. Robinson, *Surf. Sci.* **381**:L551 (1997).
15. H. L. Meyerheim, M. De Santis, W. Moritz and I. K. Robinson, *Surf. Sci.* **418**:295 (1998).
16. R. Plass and G. L. Kellogg, *Surf. Sci.* **470**:106 (2000).
17. G. Ehrlich and F. G. Hudda, *J. Chem. Phys.* **44**:1039 (1966).
18. R. L. Schwoebel and E. J. Shipley, *J. Appl. Phys.* **37**:3682 (1966).
19. D. Chatain, V. Ghetta and P. Wynblatt, *Interface Sci.* **12**:7 (2004).
20. D. Chatain, P. Wynblatt and G. S. Rohrer, *Acta Mater.* **53**:4057 (2005).
21. R. van Gastel, E. Somfai, S. B. van Saarloos and J. W. M. Frenken, *Phys. Rev. Lett.* **86**:1562 (2001).
22. M. L. Grant, B. S. Swartzentruber, N. C. Bartelt and J. B. Hannon, *Phys. Rev. Lett.* **86**:4588 (2001).
23. M. L. Anderson, M. J. D'Amato, P. J. Feibelman and B. S. Swartzentruber, *Phys. Rev. Lett.* **90**:126102/1–4 (2003).